Molecular Biology of the Cell
Vol. 18, 2755–2767, July 2007

Nitric Oxide Signaling Is Disrupted in the Yeast Model for Batten Disease[D]

Nuno S. Osório,* Agostinho Carvalho,*† Agostinho J. Almeida,*† Sérgio Padilla-Lopez,‡ Cecília Leão,* João Laranjinha,§ Paula Ludovico,* David A. Pearce,‡ and Fernando Rodrigues*

*Life and Health Sciences Research Institute (ICVS), School of Health Sciences, University of Minho, 4710 Braga, Portugal; ‡Center for Aging and Developmental Biology, Aab Institute of Biomedical Sciences, and Departments of Biochemistry and Biophysics and Neurology, University of Rochester School of Medicine and Dentistry, Rochester, NY 14642; and §Faculty of Pharmacy and Center for Neurosciences and Cell Biology, University of Coimbra, 3000 Coimbra, Portugal

Submitted November 29, 2006; Revised April 13, 2007; Accepted April 19, 2007
Monitoring Editor: Thomas Fox

The juvenile form of neuronal ceroid lipofuscinoses (JNCLs), or Batten disease, results from mutations in the CLN3 gene, and it is characterized by the accumulation of lipopigments in the lysosomes of several cell types and by extensive neuronal death. We report that the yeast model for JNCL (*btn1*-Δ) that lacks *BTN1*, the homologue to human CLN3, has increased resistance to menadione-generated oxidative stress. Expression of human CLN3 complemented the *btn1*-Δ phenotype, and equivalent Btn1p/Cln3 mutations correlated with JNCL severity. We show that the previously reported decreased levels of L-arginine in *btn1*-Δ limit the synthesis of nitric oxide (·NO) in both physiological and oxidative stress conditions. This defect in ·NO synthesis seems to suppress the signaling required for yeast menadione-induced apoptosis, thus explaining *btn1*-Δ phenotype of increased resistance. We propose that in JNCL, a limited capacity to synthesize ·NO directly caused by the absence of Cln3 function may contribute to the pathology of the disease.

INTRODUCTION

Neuronal ceroid lipofuscinoses (NCLs) are a group of inherited lysosomal storage disorders with an overall incidence of up to 1 in 12,500 live births, making it the most common type of childhood neurodegenerative disease (Goebel, 1995). The different NCL forms are characterized by massive neuronal death and accumulation of lipopigments in the lysosomes of several cell types (Goebel, 1997). Juvenile NCL (JNCL; Batten or Spielmeyer–Vogt–Sjogren disease; OMIM 204200) is the most common form, and it presents a disease course marked by vision loss, psychomotor deterioration, epileptic seizures, and premature death in the mid-20s (Boustany, 1992). JNCL is caused by mutations in CLN3, a gene identified in 1995 (Lerner *et al*., 1995). *Saccharomyces cerevisiae* harbors a gene, designated *BTN1*, that encodes a nonessential protein 39% identical and 59% similar to human Cln3 (Pearce and Sherman, 1997), and deletion of *BTN1*, *btn1*-Δ has provided a useful model for JNCL research (Pearce *et al*., 1999a,b; Kim *et al*., 2003). In *btn1*-Δ, it has been shown that pH homeostasis is altered (Pearce *et al*., 1999c) and that a decrease in vacuolar arginine transport results in a depletion of intracellular arginine levels (Kim *et al*., 2003). Expression of human Cln3 in *btn1*-Δ complemented these defects, demonstrating that the function of these proteins is conserved (Pearce *et al*., 1999c; Kim *et al*., 2003). These findings allowed the identification of primary biochemical defects in JNCL that were later confirmed in more complex animal models (Golabek *et al*., 2000; Kim *et al*., 2003; Pearce *et al*., 2003; Ramirez-Montealegre and Pearce, 2005). In spite of these and other advances in understanding the disease, an association between the known biochemical alterations and the accumulation of storage bodies or the process of neurodegeneration has not yet been established.

Oxidative stress has been widely reported in neurodegenerative conditions such as amyotrophic lateral sclerosis and Alzheimer's and Parkinson's diseases as a possible cause of cell death and as a possible effector of apoptosis (Dexter *et al*., 1989; Lassmann *et al*., 1995; Mochizuki *et al*., 1996; Beal *et al*., 1997; Smith *et al*., 1997; Good *et al*., 1998; Pedersen *et al*., 1998; Butterfield *et al*., 2002), although, in most cases, it remains unclear whether oxidative stress is the primary cause, a mediator, or a downstream consequence of the neurodegenerative process. In NCL, studies presenting increased lipid peroxidation and mitochondrial dysfunction support the hypothesis that oxidative stress might also be implicated in this pathology (Jolly *et al*., 2002; Guarneri *et al*., 2004). Nonetheless, no alterations in antioxidant enzymes were detected in several tested tissues from human patients (Marklund *et al*., 1981; Garg *et al*., 1982).

This article was published online ahead of print in *MBC in Press* (http://www.molbiolcell.org/cgi/doi/10.1091/mbc.E06–11–1053) on May 2, 2007.

[D] The online version of this article contains supplemental material at *MBC Online* (http://www.molbiolcell.org).

† These authors contributed equally to this work.

Address correspondence to: Fernando Rodrigues (frodrigues@ecsaude.uminho.pt).

Abbreviations used: ANP, D-(−)-threo-2-amino-1-[*p*-nitrophenyl]-1,3-propanediol; JNCL, juvenile neuronal ceroid lipofuscinose; L-NAME, nitro-L-arginine methyl ester; NCL, neuronal ceroid lipofuscinose; ·NO, nitric oxide; NOS, nitric-oxide synthase; ROS, reactive oxygen species.

We report that *btn1*-Δ has increased resistance to menadione indicating that a lack of Btn1p results in an increased tolerance to oxidative stress. This phenotype is specifically attributable to the lack of Btn1p, and it can be complemented by the human Cln3. Moreover, we show that this resistance to oxidative stress is a direct cause of decreased L-arginine levels in *btn1*-Δ limiting the production of nitric oxide (NO), which functions, at high concentrations, as a signal for apoptosis. Our results link a primary biochemical alteration caused by the absence of Btn1p or Cln3 with a possible mechanism of cell death. Because cell lines derived from JNCL patients also have reduced intracellular L-arginine levels (Ramirez-Montealegre *et al*., 2005), it is possible that the limitation in ·NO production we observe in *btn1*-Δ might also occur in cells from JNCL patients. Due to the importance of ·NO signaling this defect might have an important role in JNCL pathology.

MATERIALS AND METHODS

Yeast Strains and Media

S. cerevisiae strains used in this study are based in the BY wild-type reference strain purchased from Euroscarf (Frankfurt, Germany). The genetic background of the strains used is listed in Table 1. Double deletion of *SOD1/BTN1* was done by homologous recombination of a *BTN1* deletion cassette containing the hygromycin phosphotransferase (hph) gene on Y16913. Double deletion of *BTN1/SOD2* and *BTN1/CTT1* was generated by mating YO1364 with Y16605 and YO1364 with Y14718. The resulting diploid strains were sporulated and dissected. Single and double deletions were confirmed by polymerase chain reaction (PCR). Strains were maintained in YEPD agar medium containing yeast extract (0.5%, wt/vol), peptone (1%, wt/vol), glucose (2%, wt/vol), and agar (2%, wt/vol). Cells were routinely grown at 26°C with aeration on a mechanical shaker (160 rpm) in defined YNB medium containing glucose (0.5%, wt/vol) and yeast nitrogen base without amino acids (0.67%, wt/vol) supplemented with leucine, uracil, histidine, and lysine at the final concentrations of 30, 10, 5, and 5 mg/l, respectively. Growth was monitored by turbidity monitoring at 640 nm (OD_{640}) on a WPA Lightwave S2000 UV/Vis spectrophotometer (Isogen Life Science, Ijsselstein, The Netherlands). For the experimental assays, cells were grown until early logarithmic phase.

Menadione Treatments

Menadione was prepared immediately before treatment at a concentration of 10 mM in a solution of 98% ethanol, 0.2% cetrimide. Treatments were performed by direct addition of menadione solution at the indicated concentrations to cell suspensions, and controls were performed by the addition of equal volume of 98% ethanol, 0.2% cetrimide solution.

Cell Viability (Colony-forming Ability)

Cells harvested by centrifugation at 4°C (1000 × *g* for 5 min) were washed, counted, and diluted to a concentration of 3×10^6 cells/ml in 10 ml of YNB medium. Immediately before the addition of the stress agent (t0) and after different times of treatment (t*n*), 100 μl of cell suspension was diluted 1–10 three times and plated on YEPD plates. Colonies were counted after 48-h incubation at 30°C. Results of survival percentage were obtained using as reference the number of colonies counted in t0 plates versus the number of colonies obtained in t*n* plates.

Flow Cytometry Analysis

Fluorescence analysis was carried out by flow cytometry with an EPICS XL-MCL flow cytometer (Beckman Coulter, Fullerton, CA) equipped with an argon-ion laser emitting a 488-nm beam at 15 mW. The green and red fluorescence were collected through a 488-nm blocking filter, a 550-nm/long-pass dichroic with a 525-nm/band-pass and a 590-nm/long-pass with a 620-nm/band-pass, respectively. An acquisition protocol was defined to measure forward scatter (FS log), side scatter (SS log), green fluorescence (FL1 log), and red fluorescence (FL3 log) on a four-decade logarithmic scale. Data (20,000 cells/sample) were analyzed with the Multigraph software included in the system II acquisition software for the EPICS XL/XL-MCL, version 1.0.

Assessment of Intracellular Reactive Oxygen Species (ROS) Levels

Flow cytometry quantification of yeast cell populations with high ROS levels was performed after labeling with MitoTracker Red CM-H_2XRos (Invitrogen, Carlsbad, CA) as described previously (Ludovico *et al*., 2002). Briefly, cells were harvested by centrifugation, resuspended in phosphate-buffered saline (PBS), pH 7.4, and incubated for 15 min at 37°C with 50 μg/ml MitoTracker Red CM-H_2XRos. Fluorescence intensity was measured by flow cytometry, and cells displaying higher values than a defined threshold of red fluorescence were considered as containing elevated intracellular ROS levels. Epifluorescence microscopy visualization of intracellular ROS was performed after labeling with dihydrorhodamine 123 (DHR123) (Invitrogen). DHR123 was added from a 1-mg/ml stock solution in ethanol, to 5×10^6 cells/ml suspended in PBS, reaching a final concentration of 15 μg/ml. Cells were incubated during 90 min at 30°C in the dark, washed in PBS, and visualized as describe previously (Almeida *et al*., 2007). Images were acquired in an Olympus BX61 microscope with filter wheels to control excitation and emission wavelengths, equipped with a high-resolution Olympus DP70 digital camera (Olympus, Tokyo, Japan).

Plasma Membrane Integrity

Plasma membrane integrity was determined by examining cellular permeability to propidium iodide (PI) (Invitrogen), as described previously (Delafuente *et al*., 1992). Cells were incubated with 5 μg/ml PI for 15 min

Table 1. Yeast strains

Strain	Genotype	Source
Y10000 (wild type)	BY4742;MATα; his3Δ1; leu2Δ0; lys2Δ0; ura3Δ0	Euroscarf
Y11364 (*btn1*-Δ)	BY4742;MATα; his3Δ1; leu2Δ0; lys2Δ0; ura3Δ0; YJL059w::kanMX4	Euroscarf
YICVS01 (*btn1*-Δ)	BY4742;MATα; his3Δ1; leu2Δ0; lys2Δ0; ura3Δ0; YJL059w::kanMX4	This study
Y01364 (*btn1*-Δ)	BY4741;MATa; his3Δ1; leu2Δ0; met15Δ0; ura3Δ0; YJL059w::kanMX4	Euroscarf
Y12098 (*pep4*-Δ)	BY4742;MATα; his3Δ1; leu2Δ0; lys2Δ0; ura3Δ0; YPL154c::kanMX4	Euroscarf
Y10268 (*cup5*-Δ)	BY4742;MATα; his3Δ1; leu2Δ0; lys2Δ0; ura3Δ0; YEL027w::kanMX4	Euroscarf
Y16913 (*sod1*-Δ)	BY4742;MATα; his3Δ1; leu2Δ0; lys2Δ0; ura3Δ0; YJR104c::kanMX4	Euroscarf
Y12453 (*yca1*-Δ)	BY4742;MATα; his3Δ1; leu2Δ0; lys2Δ0; ura3Δ0; YOR197w::kanMX4	Euroscarf
YN0001 (denoted *pBTN1*)	BY4742;MATα; his3Δ1; leu2Δ0; lys2Δ0; ura3Δ0; YJL059w::kanMX4+pAB1795[a]	This study
YN0002 (denoted *pCLN3*)	BY4742;MATα; his3Δ1; leu2Δ0; lys2Δ0; ura3Δ0; YJL059w::kanMX4+pAB1796[a]	This study
YN0003	BY4742;MATα; his3Δ1; leu2Δ0; lys2Δ0; ura3Δ0; YJL059w::kanMX4+pAB2040[a]	This study
YN0004	BY4742;MATα; his3Δ1; leu2Δ0; lys2Δ0; ura3Δ0; YJL059w::kanMX4+pAB2041[a]	This study
YN0005	BY4742;MATα; his3Δ1; leu2Δ0; lys2Δ0; ura3Δ0; YJL059w::kanMX4+pAB2042[a]	This study
YN0006	BY4742;MATα; his3Δ1; leu2Δ0; lys2Δ0; ura3Δ0; YJL059w::kanMX4+pAB2043[a]	This study
YN0007	BY4742;MATα; his3Δ1; leu2Δ0; lys2Δ0; ura3Δ0; YJL059w::kanMX4+pAB2044[a]	This study
YN0008	BY4742;MATα; his3Δ1; leu2Δ0; lys2Δ0; ura3Δ0; YJL059w::kanMX4+pAB2045[a]	This study
YN0010	BY4742;MATα; his3Δ1; leu2Δ0; lys2Δ0; ura3Δ0; YJL059w::kanMX4+pAA1037[a]	This study
YICVS02 (*sod1*-Δ*btn1*-Δ)	BY4742;MATα; his3Δ1; leu2Δ0; lys2Δ0; ura3Δ0; YJR104c::kanMX4; YJL059w::hph	This study

[a] The plasmids used are described in Pearce and Sherman (1998).

and analyzed by flow cytometry or epifluorescence microscopy. Heat-killed cells were used as a positive control. Cells displaying higher values than a defined threshold of red fluorescence were considered as having compromised plasma membrane integrity.

Assessment of Mitochondrial Function and Integrity

The charged cationic green dye rhodamine 123 (Invitrogen) was used to assess mitochondrial function/integrity as described previously (Ludovico *et al*., 2001). Cells were harvested by centrifugation and incubated with 25 μg/ml rhodamine 123 for 15 min at 37°C. Fluorescence intensity was measured by flow cytometry, and cells displaying higher values than a defined threshold of green fluorescence were considered has having compromised mitochondrial or functional integrity.

Enzyme Activity Assays

Cells were harvested, washed, and resuspended in 2 ml of 0.05 M phosphate buffer. To disrupt cells, 200 μl of 0.5-mm-diameter glass beads was added, and sonication for 10 times in 30-s intervals interspersed with periods of cooling in ice. Cellular debris was removed by a 15-min centrifugation at 15,000 × *g*, and the supernatant was collected. Protein concentration was determined using the Bradford method using bovine serum albumin as standard. Superoxide dismutase activity was expressed in units defined as the enzyme amount able to inhibit in 50% the velocity of cytochrome *c* reduction per minute and milligrams of total protein according to McCord and Fridovich (1969). Glucose-6-phosphate dehydrogenase (G6PDH) activity was based on the increase in absorbance at 340 nm, resulting from NADP reduction, as described previously (Postma *et al*., 1989).

·NO Measurements

Kinetics of ·NO production and decay was measured using an ·NO-selective carbon fiber microelectrode coated with Nafion and *o*-phenylenediamine as described previously (Ledo *et al*., 2002; Ferreira *et al*., 2005). Early log cells (9×10^8) were washed, resuspended in 2 ml of 10 mM Tris-HCl, pH 7.4, and transferred to a recording cell with agitation under aerobic conditions. Amperometric currents originated from the oxidation of ·NO at the electrode surface were recorded by differential pulse amperometry (between +0.7 and +0.9 V, the range that includes the oxidation peak of ·NO for the experimental conditions used) using on a PGSAT 12 potentiostat (EcoChimie, Utrecht, The Netherlands) with low current module installed and controlled by GPES software, version 4.9 (EcoChimie), by using a three-electrode system with a platinum wire auxiliary electrode, a silver/silver chloride (3 M) reference electrode, and the ·NO-selective carbon fiber electrode as the working electrode. The electrodes were calibrated by a single stream flow injection analysis system using ·NO solutions prepared from ·NO donor (diethylenetriamine-NO) or from ·NO gas, as described previously (Ferreira *et al*., 2005). The intracellular levels of ·NO were assessed using the ·NO-selective probe 4-amino-5-methylamino-2′,7′-difluorofluorescein (DAF-FM) (Invitrogen). Cells were harvested, washed, and resuspended in PBS, pH 7.4, and incubated for 15 min at 37°C with 5 μg/ml DAF-FM. The mean fluorescence intensity of 20,000 cells per sample was measured by flow cytometry.

Quantification of Intracellular Levels of L-Arginine

A standard procedure for extraction of total amino acids was used (Ohsumi *et al*., 1988). In summary, cells at OD_{600} of 0.6 were harvested, washed twice in distilled water, resuspended in AA buffer (2.5 mM potassium phosphate buffer, pH 6.0, 0.6 M sorbitol, 10 mM glucose, and 0.2 M $CuCl_2$) and incubated for 10 min at 30°C. The cell suspension was collected by filtration on 0.45-μm membrane filters (Millipore, Billerica, MA) and washed four times with AA buffer lacking 0.2 M $CuCl_2$, representing the cytosolic fraction (Ohsumi *et al*., 1988). Cells retained on the filters were resuspended in water, boiled for 15 min, and then centrifuged at 5000 × *g* for 5 min. The supernatant was collected as the vacuolar fraction. Both fractions were combined, and homoserine was added as an internal control. Arginine concentration was then measured using high-performance liquid chromatography following the manufacturer's protocol (ESA, Boston, MA).

Nucleic Markers of Programmed Cell Death

Study of nuclear morphological alterations was performed by staining with 4′,6-diaminilo-2-phenylindol dihydrochloride (DAPI). Cells were harvested, washed, and then resuspended in PBS, pH 7.4, and incubated for 10 min at 37°C with 0.5 μg/ml DAPI. Stained cells were washed twice with PBS and visualized by epifluorescence microscopy (Auxioskop 2 Plus; Carl Zeiss, Jena, Germany). DNA strand breaks were demonstrated by terminal deoxynucleotidyl transferase dUTP nick-end labeling (TUNEL) assay with the In Situ Cell Death Detection kit, fluorescein (Roche Diagnostics, Indianapolis, IN).

Assessment of Caspase-like or ASPase Activity

Study of yeast caspase-like or other ASPase activity was performed using CaspSCREEN Flow Cytometric Analysis kit (Chemicon International, Temecula, CA). Briefly, cells were incubated with the nonfluorescent substrate $(Asp)_2$-rhodamine 110 (D_2R) at 37°C for 45 min, and then they were analyzed by flow cytometry. Cells displaying higher values than a defined threshold of fluorescence were considered has presenting caspase-like or other ASPase activity (Vachova *et al*., 2005; Almeida *et al*., 2007).

RESULTS

btn1-Δ Has Increased Resistance to Oxidative Stress

To study a possible role of oxidative stress in JNCL, we screened *btn1*-Δ cells sensitivity to oxidative stress induced by several prooxidant agents. Strains deleted in *BTN1* (for details, see Table 1) presented increased resistance to menadione (Figure 1A), diamide, and hydrogen peroxide (see Supplemental Material) compared with wild-type cells. The most marked differences were obtained for menadione treatment, in which considerable loss of *btn1*-Δ cells viability was only obtained for concentrations >0.1 mM, whereas wild-type cells were severely affected by lower menadione concentrations, presenting <10% of viability when treated with 0.1 mM.

To determine whether *BTN1* and the human CLN3 could complement the described phenotype, we determined the viability of *btn1*-Δ mutants expressing either gene. Expression of *BTN1* or CLN3 in *btn1*-Δ strain (denoted pBTN1 and pCLN3, respectively) decreased the viability after menadione treatment of these strains to the wild-type level (Figure 1B), indicating the dependence of the resistance phenotype on the lack of *BTN1*/CLN3. The first report showing a Btn1p-specific phenotype in yeast was the increased *btn1*-Δ resistance to D-(−)-threo-2-amino-1-[*p*-nitrophenyl]-1,3-propanediol (ANP), a breakdown product of chloramphenicol with pH-dependent toxicity (Pearce and Sherman, 1998), allowing the finding of altered pH homeostasis in *btn1*-Δ. This study also establishes parallels between fundamental biological processes in yeast and characteristics in

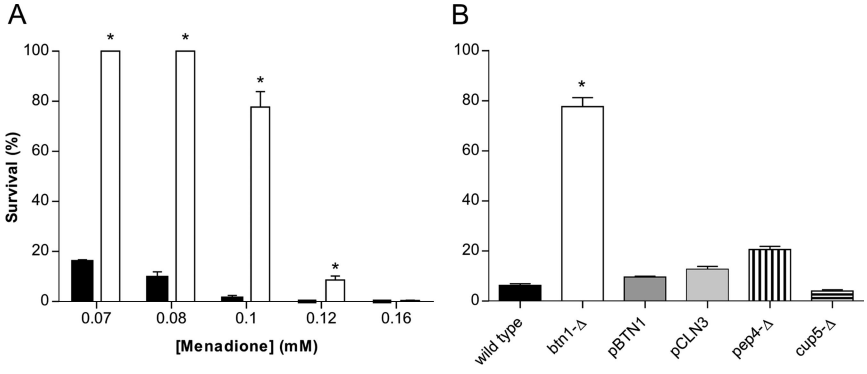

Figure 1. Effect of 200-min menadione treatment on the survival of the wild-type, *btn1*-Δ, and other mutant strains cells. (A) Percentage of survival of wild-type (closed bars) and *btn1*-Δ (open bars) cells after treatment with increasing concentrations of menadione ranging from 0.07 to 0.16 mM. (B) Survival after treatment with 0.1 mM menadione of *btn1*-Δ cells expressing BTN1(pBTN1) and the human CLN3(pCLN3) and cells deleted in the vacuolar aspartyl protease Pep4p (*pep4*-Δ) and in the subunit of the vacuolar H^+-ATPase Cup5p (*cup5*-Δ). *p ≤ 0.001 versus wild-type, *t* test; n = 5.

Table 2. Correlation between the severity of different JNCL disease variants (Munroe *et al*., 1997) and the percentage of survival to menadione treatment of yeast strains with the corresponding alterations

Cln3 (human)		Btn1p (yeast)		
Alteration	Severity of JNCL variant	Alteration	Survival (%) after 200-min 0.1 mM menadione	ANP resistance
None	0	None	9.88 ± 1.23	0
R334H	3	R293H	56.34 ± 2.43	2
L101P	2	L44P	52.30 ± 1.99	2
L170P	1	L112P	31.78 ± 2.06	0
E295K	1	E243K	29.88 ± 1.09	0
V330F	3	V289F	32.12 ± 2.06	1
R334C	3	R293C	79.06 ± 4.28	2
Deletion	3	Deletion	83.41 ± 1.61	3

The indicated values for percentage of survival are the mean of at least three independent assays, and SD resistance to ANP described by Pearce and Sherman (1998) is also included.

the human disease by correlating the increased resistance of *btn1*-Δ to ANP and the severity of JNCL. To further evaluate the relationship between higher resistance to menadione and the function of Btn1p, we tested the menadione sensitivity of several *btn1*-Δ strains expressing Btn1p with the following amino acid replacements: R293H, L44P, L112P, E243K, V289F, and R293C. These mutations are the counterparts of a spectrum of Cln3 mutations known to occur in the human disease heterozygously with the most frequent 1.02-kb deletion (GenBank X99832). The degree of *btn1*-Δ menadione resistance is decreased by the expression of mutated Btn1p, and for the majority of these mutations, the degree of menadione resistance can be correlated with JNCL severity (Table 2).

Btn1p has been shown to be a vacuolar protein (Pearce *et al*., 1997; Croopnick *et al*., 1998). To test whether *btn1*-Δ increased menadione resistance was specific to *btn1*-Δ and not an effect attributable to general vacuolar dysfunction, we determined the viability of strains harboring deletions in other vacuolar proteins, namely, Cup5p (a subunit of the vacuolar H^+-ATPase) and Pep4p (a vacuolar aspartyl protease). Both *cup5*-Δ and *pep4*-Δ strains display low resistance to menadione similar to the wild-type control (Figure 1B).

Increased btn1-Δ Menadione Resistance Is Associated with Lower ROS Levels

Treatment with menadione induces the catalytic reduction of oxygen to superoxide and other ROS, triggering mild-to-severe cellular damage and ultimately cell death (Thor *et al*., 1982; Morrison *et al*., 1984). For additional characterization of the *btn1*-Δ phenotype, we performed the analysis of intracellular ROS levels, cell death, plasma membrane integrity, and mitochondrial function/integrity along 200-min treatment with 0.1 mM menadione (Figure 2, A–D). A slow increase in the percentage of *btn1*-Δ cells with elevated endogenous ROS, resulting in a mean value of 45.2% of cells with a positive response at the end of the treatment, was observed. In contrast, the wild-type strain showed an abrupt increase in cells with elevated intracellular ROS with a mean value of 74.7% after 60-min treatment and 97.3% after 120 min (Figure 2A). These data correlate with the kinetic analysis of cell death in which the slow death rate of *btn1*-Δ cells was markedly different from the obtained for the wild-type strain where <10% survival was observed after 120-min treatment (Figure 2B). At this time point, the entire wild-type population presented compromised plasma membrane integrity, whereas only 44.9% of *btn1*-Δ cell population had lost membrane integrity (Figure 2C). Rh123 cell staining showed that *btn1*-Δ strain displayed reduced percentages of cells with defective mitochondrial function/integrity at the later stages of treatment compared with the wild-type strain (Figure 2D). To assess whether the differences in intracellular ROS levels between *btn1*-Δ and wild-type cells preceded loss of cellular integrity and cell death, we visualized cells colabeled with DHR123 and PI after 30 min of menadione treatment (≈70% viability in wild-type cells). The results show that live wild-type cells with preserved membrane integrity present increased intracellular ROS levels when compared with *btn1*-Δ cells (Figure 2E), suggesting the presence of a different ROS metabolism in both strains. Therefore, to evaluate whether the lower levels of ROS in *btn1*-Δ cells were due to an increased detoxification capacity, we have performed an evaluation of antioxidant defenses. No significant alterations in the activity of superoxide dismutases were detected when comparing *btn1*-Δ and wild-type cells (Table 3). The activity of catalase was also not altered in *btn1*-Δ cells, even though it could only be detected in stationary phase (data not shown). Additionally, we studied whether differences in glutathione synthesis and redox balance were involved in the *btn1*-Δ phenotype. The viability of *btn1*-Δ and wild-type strains was largely reduced when cells with inhibited glutathione biosynthesis were treated with 0.1 mM menadione (see Supplemental Material). However, when using lower menadione concentrations, the differences in resistance between both strains were maintained (see Supplemental Material), indicating that glutathione synthesis is not accountable for *btn1*-Δ phenotype. In addition, the activity of glucose-6-phosphate dehydrogenase, the major source of NADPH necessary for the redox balance of glutathione in yeast (Nogae and Johnston, 1990) was similar in both strains (Table 3). These results are in accordance with the data from DNA microarray analysis of *btn1*-Δ strain that shows no differential expression of genes encoding for enzymes involved in ROS detoxification (Pearce *et al*., 1999a).

btn1-Δ Has Reduced ·NO Production, Impairing Oxidative Signaling

Several studies suggest that ·NO may enhance intracellular ROS generation (Zamzami *et al*., 1995; Packer *et al*., 1996). Moreover, L-arginine, the substrate of the ·NO synthesis, is decreased in *btn1*-Δ cells (Kim *et al*., 2003), leading to the hypothesis that the reduced ROS levels of *btn1*-Δ are associated to an impairment in ·NO synthesis. Because the synthesis of ·NO by yeast cells is still poorly studied, we first assessed whether nitric-oxide synthase (NOS)-like activity could be detected in *S. cerevisiae*. Using a standard NOS activity assay, we were able to detect conversion of arginine to citrulline in yeast protein extract, partially inhibited by 1 mM nitro-L-arginine methyl ester (L-NAME) (see Supplemental Material). Additionally, using an ·NO-selective electrode, we measured that yeast cells produce ·NO in response to menadione, and we found that ·NO production was enhanced by L-arginine (and not by its inactive enantiomer D-arginine; data not shown) and that it was inhibited by L-NAME (Figure 3A). Together, these findings suggest that an enzyme with NOS-like activity may exist in yeast. We then studied the levels of ·NO production in *btn1*-Δ cells. Our results indicate that the production of ·NO in response to menadione treatment is decreased in *btn1*-Δ. Importantly, this defective ·NO production in *btn1*-Δ can be overcome by

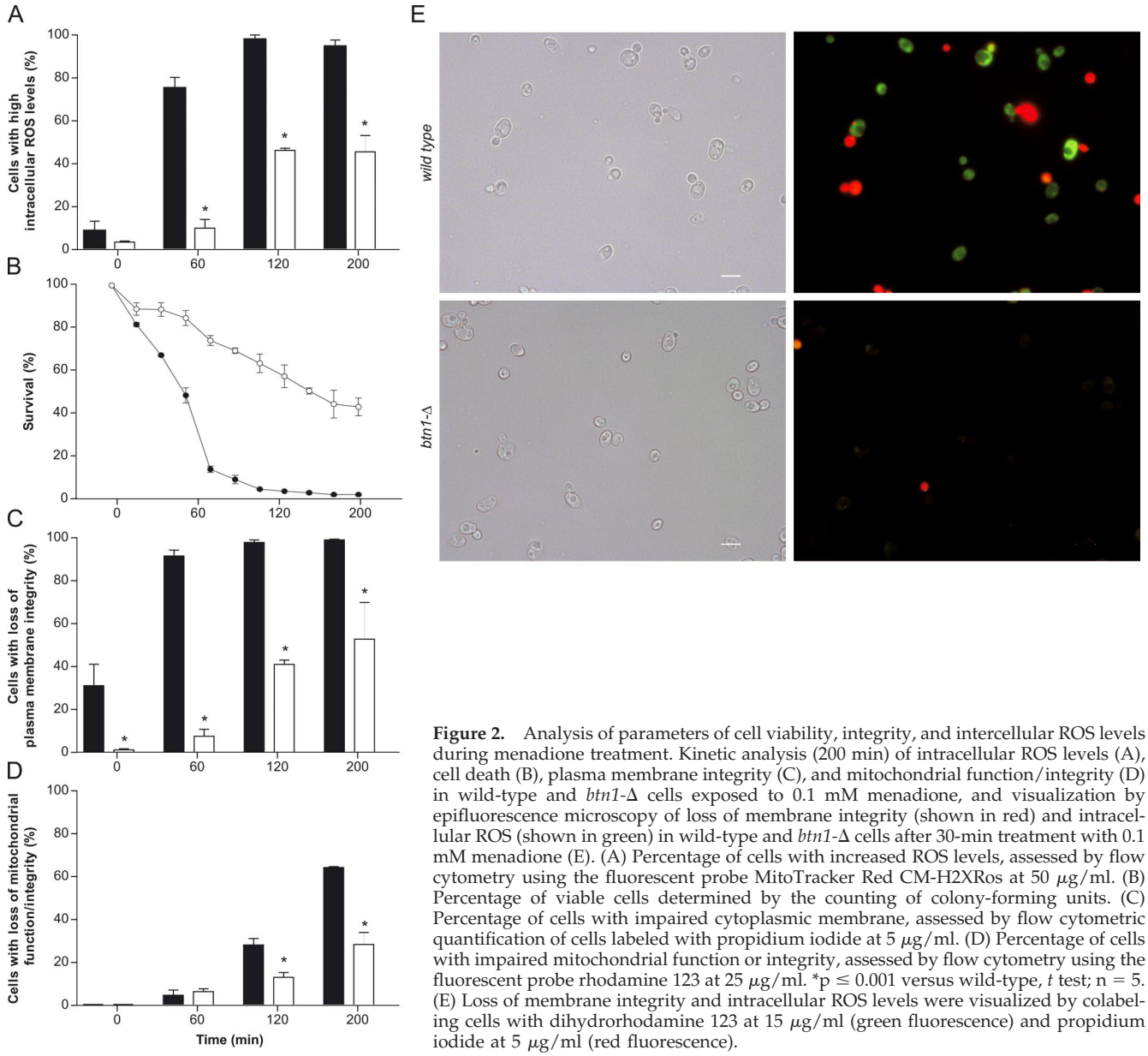

Figure 2. Analysis of parameters of cell viability, integrity, and intercellular ROS levels during menadione treatment. Kinetic analysis (200 min) of intracellular ROS levels (A), cell death (B), plasma membrane integrity (C), and mitochondrial function/integrity (D) in wild-type and *btn1*-Δ cells exposed to 0.1 mM menadione, and visualization by epifluorescence microscopy of loss of membrane integrity (shown in red) and intracellular ROS (shown in green) in wild-type and *btn1*-Δ cells after 30-min treatment with 0.1 mM menadione (E). (A) Percentage of cells with increased ROS levels, assessed by flow cytometry using the fluorescent probe MitoTracker Red CM-H2XRos at 50 μg/ml. (B) Percentage of viable cells determined by the counting of colony-forming units. (C) Percentage of cells with impaired cytoplasmic membrane, assessed by flow cytometric quantification of cells labeled with propidium iodide at 5 μg/ml. (D) Percentage of cells with impaired mitochondrial function or integrity, assessed by flow cytometry using the fluorescent probe rhodamine 123 at 25 μg/ml. *$p \leq 0.001$ versus wild-type, *t* test; n = 5. (E) Loss of membrane integrity and intracellular ROS levels were visualized by colabeling cells with dihydrorhodamine 123 at 15 μg/ml (green fluorescence) and propidium iodide at 5 μg/ml (red fluorescence).

the addition of L-arginine, strongly suggesting that the impairment in L-arginine homeostasis in *btn1*-Δ underlies this signaling defect. This result was corroborated by the use of a fluorescent probe selective for ·NO, DAF-FM (Figure 3B).

Table 3. Enzyme-specific activities

	Specific activity (U mg^{-1} protein)	
Enzyme	Wild type	*btn1*-Δ
Total superoxide dismutase (SOD)	6.29 ± 0.84	5.50 ± 0.43
Mn-SOD	3.73 ± 0.30	4.25 ± 0.39
Cu, Zn-SOD	2.57 ± 0.54	1.25 ± 0.90
G6PDH	$47.03 \times 10^{-3} \pm 2.58 \times 10^{-3}$	$47.62 \times 10^{-3} \pm 0.69 \times 10^{-3}$

The activity was measured in cell-free extract of both wild-type and *btn1*-Δ cells grown in YNB liquid medium and harvested in the exponential phase of growth. Indicated activity values are the mean of at least three assays and corresponding SD. No significant differences were found by *t* test comparing the specific activity of each studied enzyme in wild-type versus *btn1*-Δ cells.

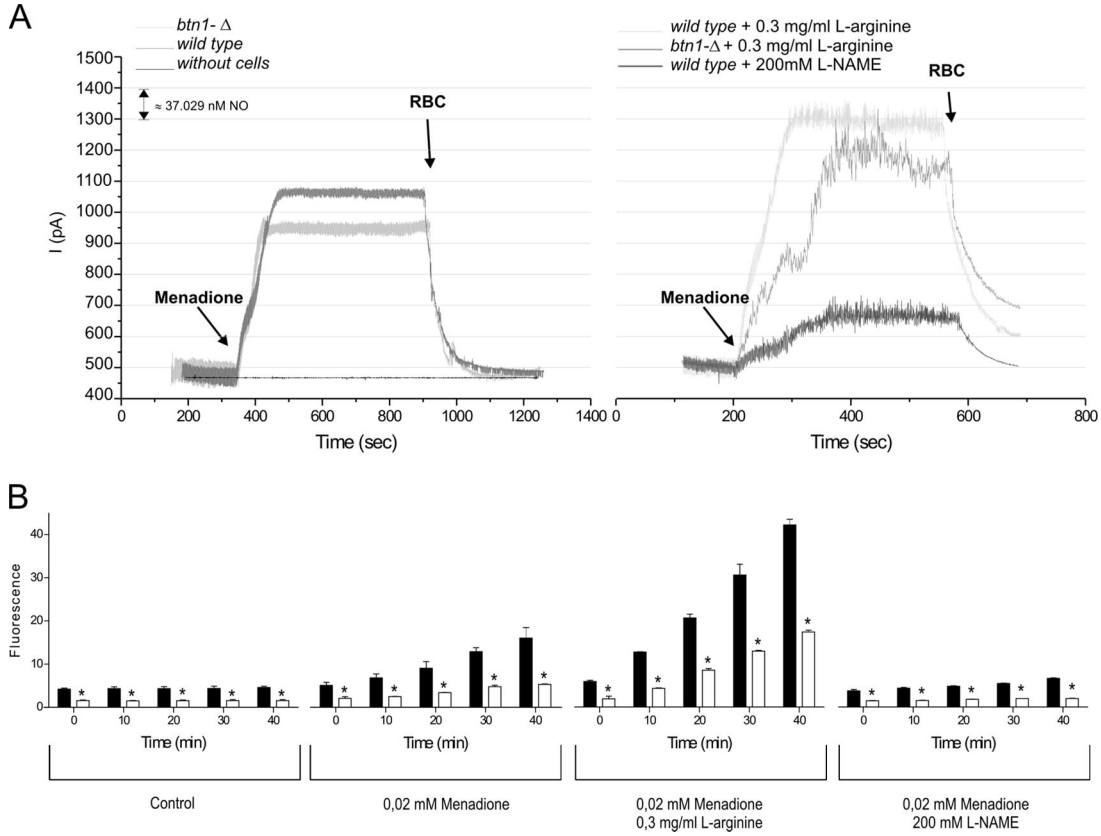

Figure 3. Measurement of ·NO production in wild-type and *btn1*-Δ cells. (A) Typical recording of ·NO production using an ·NO-selective electrode after the addition of 0.1 mM menadione to 9×10^8 wild-type and *btn1*-Δ cells in the presence or absence of 0.3 mg/ml L-arginine and with or without preincubation with 200 mM of L-NAME. An increase of 100 pA corresponds to a production of ~37 nM ·NO. The signal was quenched by the addition of 150 μl of packed red blood cells (RBC). (B) Forty-minute kinetic quantification by flow cytometry of the mean fluorescence intensity of wild-type (closed bars) and *btn1*-Δ (open bars) cells stained with DAF-FM, a probe specific for ·NO, in physiological conditions, after treatment with 0.02 mM menadione and after the same menadione treatment in the presence of 0.3 mg/ml L-arginine or 200 mM L-NAME. *$p \leq 0.05$ versus wild type, *t* test; n = 3.

In addition, this methodology allowed detecting significant lower ·NO levels under physiological conditions when comparing *btn1*-Δ to wild-type cells (Figure 3B). Furthermore, the analysis of *btn1*-Δ and *btn1*-Δ strains expressing mutated Btn1p showed different ·NO levels that could be directly correlated with the different intracellular arginine levels present in each strain (Figure 4). Collectively, these data imply that the defective arginine levels caused by the lack

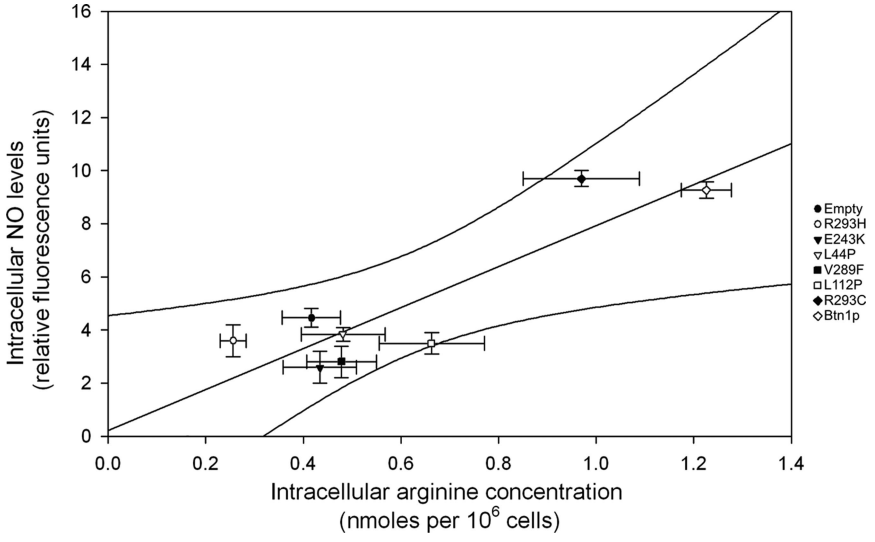

Figure 4. Correlation between the intracellular ·NO levels detected by labeling cells with DAF-FM and intracellular arginine levels measured by HPCL in *btn1*-Δ strains transformed with the empty plasmid and plasmids allowing expression of normal and point mutated Btn1p. The linear regression graph shows results for each strain with SE and 99% confidence interval for n ≥ 3.

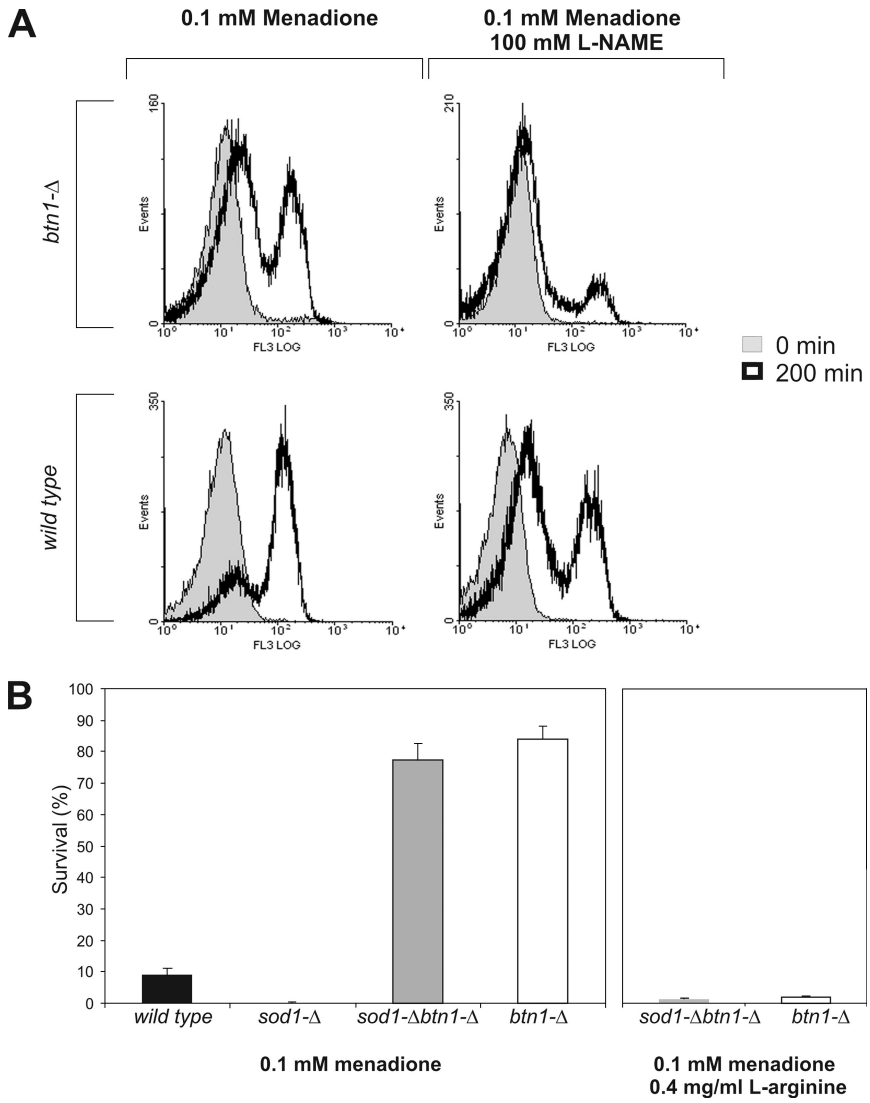

Figure 5. Role of ROS in menadione-induced cell death. (A) Flow cytometric study of the production of ROS in wild-type and *btn1*-Δ cells stained with 50 μg/ml Mito-Tracker Red CM-H2XRos after 200-min treatment with 0.1 mM menadione in the presence and absence of 100 mM L-NAME. The data are presented in the form of representative frequency histograms displaying relative fluorescence (*x*-axis) against the number of analyzed events (*y*-axis). (B) Survival after 200-min treatment with 0.1 mM menadione of wild-type, *btn1*-Δ, *sod1*-Δ, *sod1*-Δ *btn1*-Δ cells in the presence or absence of 0.4 mg/ml L-arginine.

of Btn1p function disrupt endogenous ·NO production in yeast.

To study whether the endogenous production of ROS in yeast cells upon menadione treatment was influenced by ·NO, we measured the intracellular ROS levels in both strains after menadione treatment in the presence of L-NAME. Our results show that in the presence of L-NAME, the subpopulation of cells with high levels of ROS is largely decreased in both strains (Figure 5A). This is indicative that ROS generation upon menadione treatment is partially dependent of endogenous ·NO production. To further test this hypothesis, we have used a strain, *sod1*-Δ, that has <90–95% of the total wild-type superoxide dismutase activity; and for this reason, it is highly sensitive to redox cycling compounds (Gralla, 1997), including menadione (Figure 5B). Most interestingly, the deletion of *BTN1* within *sod1*-Δ background resulted in a marked survival increase after menadione treatment to values similar to *btn1*-Δ cells (Figure 5B). This increased resistance of *sod1*-Δ *btn1*-Δ cells was lost when treatment was performed in the presence of L-arginine (Figure 5B). Deletion of *BTN1* in strains lacking other ROS detoxifying enzymes, namely, *sod2*-Δ and *ctt1*-Δ also resulted in increased survival rates to menadione treatment that were reverted by L-arginine addition (data not shown). Collectively, these results suggest that the deletion of *BTN1* causes a high decrease in the production of intracellular ROS after menadione treatment to levels that are tolerated even in

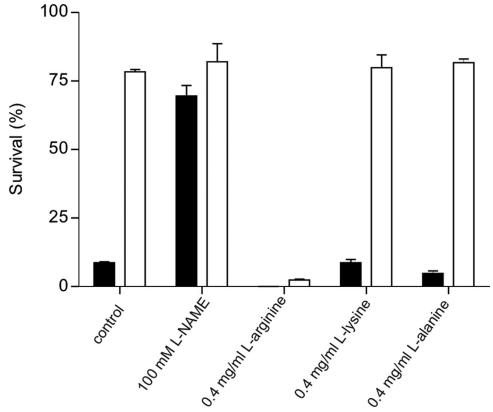

Figure 6. Percentage of viable cells after 200-min treatment with 0.1 mM menadione in wild-type (closed bars) and *btn1*-Δ (open bars) cells after 1-h pretreatment with 100 mM L-NAME, 0.4 mg/ml L-arginine, 0.4 mg/ml L-lysine, and 0.4 mg/ml L-alanine. *$p \leq 0.001$ versus wild type, *t* test; n = 3.

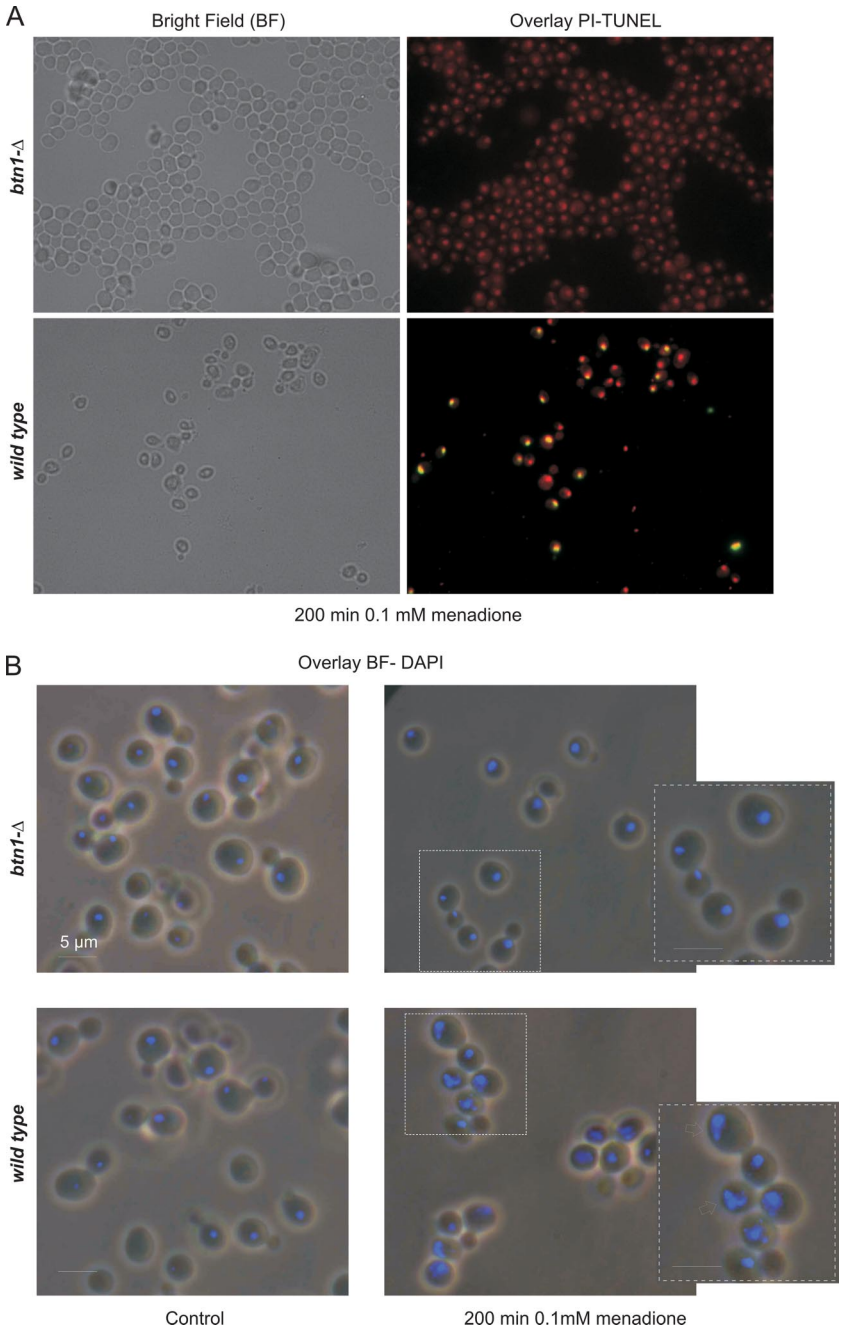

Figure 7. Determination of nuclear markers of apoptosis by fluorescence microscopy in wild-type and *btn1*-Δ cells after 200-min treatment with 0.1 mM menadione. (A) Cells visualized after TUNEL staining; the yellow fluorescence observed in the wild-type cells results from the colocalization of the red probe specific for double-stranded nucleic acids and the green probe that marks DNA breaks. (B) Cells visualized after DAPI staining, the arrows point to characteristic programmed cell death alterations observed in the wild type, such as chromatin condensation and nuclear fragmentation.

the absence of Sod1p. This phenotype was reverted by L-arginine, suggesting that ·NO was mediating a burst of intracellular ROS production after menadione stimulus. To study the relevance of ·NO signaling in the response to menadione, we tested the viability after menadione treatment of *btn1*-Δ and wild-type cells in the presence of L-NAME or L-arginine. Interestingly, wild-type cells showed a sevenfold increase in viability when preincubated with L-NAME, reaching values similar to *btn1*-Δ (Figure 6). In contrast, incubation with L-arginine before menadione treatment resulted in a marked decrease in *btn1*-Δ survival to values similar to those obtained for menadione treated wild-type cells (Figure 6). No effect in the growth rate of either strain was obtained in media supplemented with this concentration of L-arginine (data not shown). Additionally, to test the specificity of L-arginine effect on menadione-induced apoptosis, viability of both strains was assayed after menadione treatment in the presence of similar concentrations of L-alanine or L-lysine. These amino acids had no effect on survival rates (Figure 6), suggesting that the observed phenomenon is specific of L-arginine.

Defective ·NO Production Inhibits Menadione-induced Apoptosis in btn1-Δ

In a dose-dependent manner, menadione is known to induce apoptosis in eukaryotic cells, and reactive oxygen and nitrogen species are thought to be important mediators in this process (Madeo *et al*., 1999; Gerasimenko *et al*., 2002; Chen *et al*., 2003). The increased resistance of *btn1*-Δ cells and the reduced levels of ·NO and ROS found in this strain after

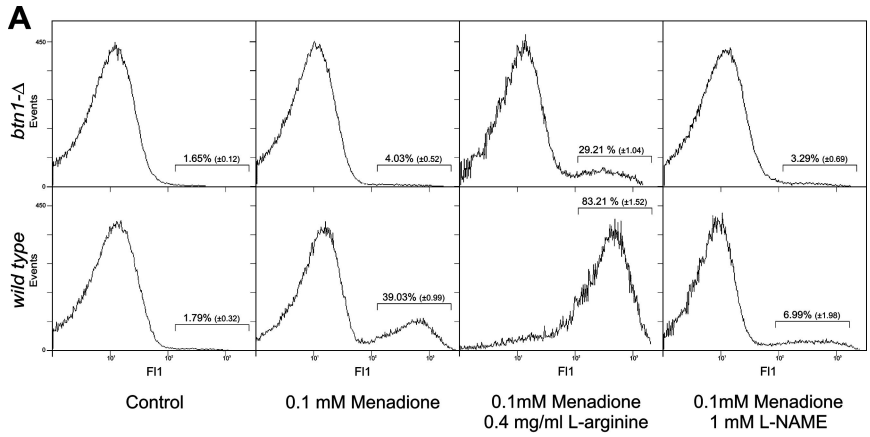

Figure 8. Role of yeast metacaspase in menadione-induced cell death. (A) Measurement of intracellular caspase-like activity (or other protease able to cleave substrates after Asp residue; ASPase) by the use of D_2R in wild-type and *btn1*-Δ cells after 200-min treatment with 0.1 mM menadione in the presence or absence of 100 mM L-NAME and 0.3 mg/ml L-arginine. The data are presented in the form of frequency histograms displaying relative fluorescence (*x*-axis) against the number of events analyzed (*y*-axis). (B) Viability of cells deleted in the metacaspase YCA1 after 200-min treatment with 0.1 mM menadione.

menadione treatment led us to question whether menadione-induced apoptosis was impaired in *btn1*-Δ cells. Menadione-treated cells were examined for nuclear markers of apoptosis such as DNA fragmentation and alterations in nuclear morphology. No DNA fragmentation could be observed in *btn1*-Δ cells by TUNEL assay, whereas several wild-type cells presented a TUNEL-positive phenotype, indicative of the presence of fragmented DNA (Figure 7A). Furthermore, no nuclear morphological alterations were detected in *btn1*-Δ cells after menadione treatment, whereas wild-type cells showed typical apoptotic nuclear alterations (Figure 7B), suggesting that menadione-induced apoptosis is largely impaired in *btn1*-Δ cells. We also tested the involvement of yeast metacaspase activation (Madeo *et al*., 2002) in menadione-induced cell death. We measured ASPase activity in *btn1*-Δ and wild-type cells by flow cytometric analysis of cells labeled with the substrate D_2R, which was shown to become fluorescent only after cleavage by ASPase activity in yeast cells (Vachova *et al*., 2005; Almeida *et al*., 2007). Menadione treatment induced a subpopulation of ~39% of wild-type cells with high fluorescence, indicative of ASPase activity, whereas no significant activity was detected in *btn1*-Δ cells (Figure 8A). Additionally, ASPase activity seems to be dependent on ·NO production, because the treatment with menadione in the presence of L-arginine resulted in an increase in percentage of wild-type and *btn1*-Δ cells with positive staining, whereas L-NAME decreased the positive subpopulation. Furthermore, the survival to menadione treatment of cells deleted in yeast metacaspase (*yca1*-Δ) is significantly increased compared with the survival of wild-type cells (Figure 8B). These results suggest that yeast metacaspase is involved in menadione-induced apoptosis and that *btn1*-Δ cells are unable to activate yeast metacaspase, possibly due to the ·NO production defect.

DISCUSSION

We report that *btn1*-Δ results in an increased resistance to oxidative stress induced by several prooxidant agents, including menadione. These data describe a new phenotype specifically attributable to the lack of *BTN1*, because it is complemented by the expression of Btn1p. Phenotypic complementation also results from expression of the human Cln3, representing additional evidence of high functional conservation between Btn1p and Cln3. Similarly to a previous report on increased resistance of *btn1*-Δ to ANP (Pearce *et al*., 1998), a correlation between JNCL severity and menadione resistance was obtained for most of the corresponding Btn1p/Cln3 mutations. The potential of this type of analysis is largely affected by the difficulties in evaluating the severity of the disease and by the reduced number of JNCL patients that are compound heterozygous. Nonetheless, these data constitute important validation of the model.

Menadione, is a quinone that induces toxicity mainly by redox cycling that consists in the catalytic reduction of oxygen to superoxide anion and other reactive oxygen species (Thor *et al*., 1982). Interestingly, following menadione treatment *btn1*-Δ cells show decreased levels of intracellular ROS, while presenting no significant increases in the major ROS detoxification systems compared with wild-type cells. Because L-arginine, the substrate in ·NO synthesis pathway, is decreased in *btn1*-Δ cells (Kim *et al*., 2003) and ·NO may have a role in enhancing ROS generation within the cell (Zamzami *et al*., 1995; Packer *et al*., 1996; Boveris *et al*., 2000), it was questioned whether ·NO was being produced in response to menadione treatment and whether it was involved in *btn1*-Δ menadione-resistance phenotype. We have shown that yeast cells produce ·NO in response to oxidative stress generated by menadione by the use of both a selective electrode and an

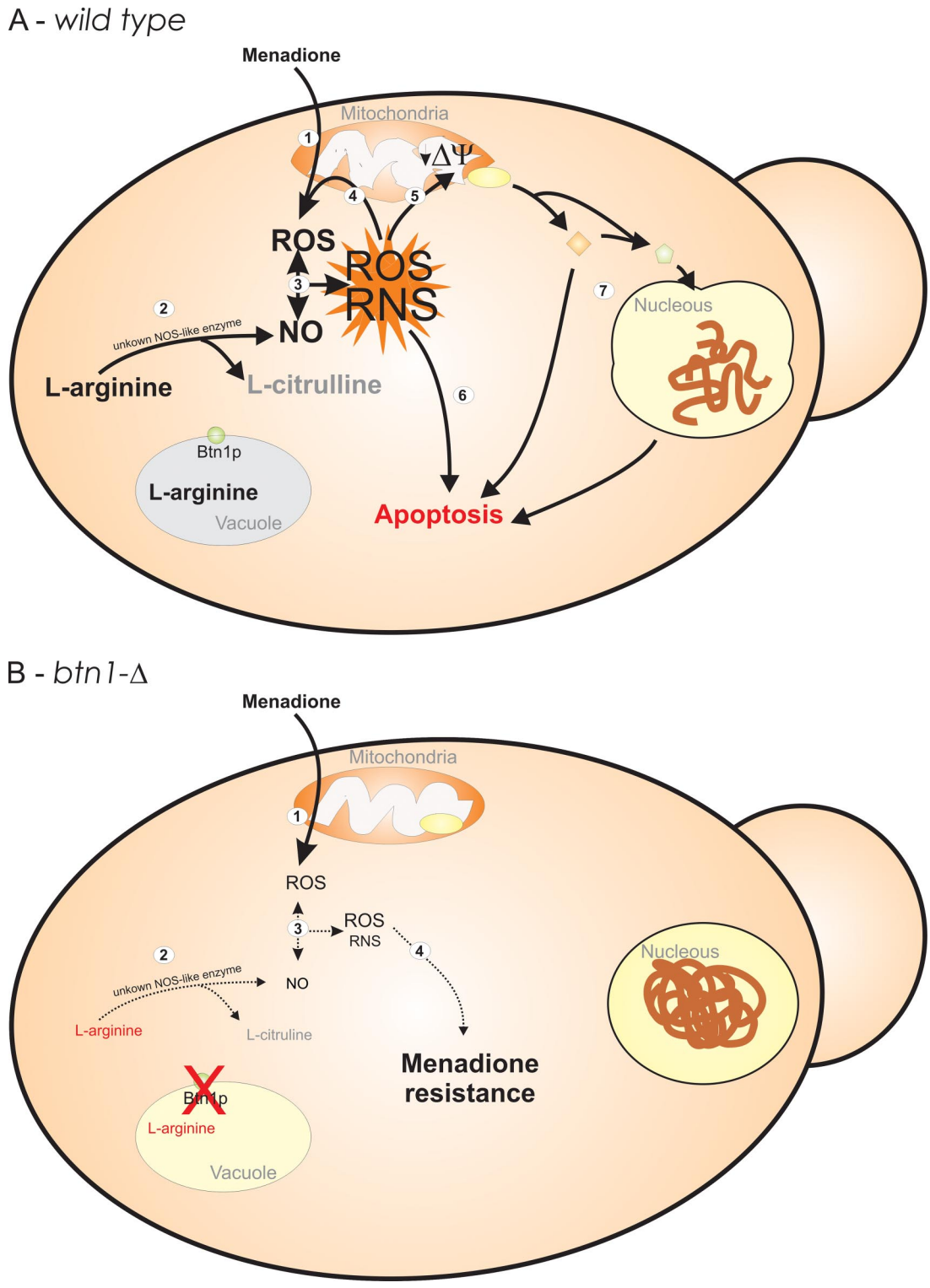

Figure 9. Schematic model of response to menadione treatment of wild-type (A) and *btn1*-Δ (B) cells. Menadione treatment of wild-type cells (1) induces toxicity by redox cycling, generating superoxide anion and other ROS and triggering endogenous ·NO production (2). The reaction between ·NO and superoxide anion results in the formation of other reactive species, such as peroxynitrite (3). These species can cause increased generation of ROS in the mitochondria (Zamzami *et al.*, 1995; Packer *et al.*, 1996), amplifying the activation of cell death pathways (4–7). Another consequence of mitochondrial damage can be the loss of mitochondrial membrane potential (5) and the release of proapoptotic molecules that activates caspases and other cell death effectors (Brune, 2005) (7). The absence of Btn1p causes altered vacuolar pH (Pearce *et al.*, 1999c) and reduced intracellular levels of L-arginine (Kim *et al.*, 2003). The ROS generated by menadione redox cycling in *btn1*-Δ cells (1) results in insufficient endogenous ·NO production due to L-arginine limitation (2). The milder concentrations of ·NO generated and the consequent lower levels of ROS and reactive nitrogen species (RNS) formed are insufficient to induce the activation of mitochondrial cell death pathways impairing the apoptotic process (3 and 4).

·NO-sensitive fluorescent probe. This finding is consistent with studies on the function of yeast flavohemoglobin (Yhb1p) that imply the production of ·NO in response to oxidative stress (Cassanova *et al*., 2005). Our results also show that the production of ·NO is enhanced by L-arginine and inhibited by L-NAME, and we were able to detect conversion of radioactive-labeled arginine to citrulline in yeast protein extracts. Together, these results suggest enzymatic production of ·NO from L-arginine. Previous studies suggest that *S. cerevisiae* produces ·NO by a mechanism similar to a classical NOS (Kanadia *et al*., 1998; Domitrovic *et al*., 2003). However, bioinformatic analysis of the *S. cerevisiae* genome fails to identify sequences that are homologous to known NOS (data not shown). Thus, it is likely that *S. cerevisiae* has an unknown enzyme with NOS-like activity that is structurally unrelated to classical NOS, similarly to what has been observed in plants (Guo *et al*., 2003). A recent study shows that yeast cells generate ·NO from nitrite in hypoxic conditions in a manner dependent from mitochondrial respiratory chain that is consequently abolished by cyanide (Castello *et al*., 2006). Contrarily, the blockage of mitochondrial respiratory chain by cyanide did not alter ·NO production and cell survival after menadione treatment of wild-type and *btn1*-Δ cells (data not shown), indicating an ·NO production process distinct from that described by Castello and coworkers. Menadione-induced ·NO production seems to be an essential upstream cell death signal, because the inhibition of ·NO production by L-NAME treatment decreases the intracellular ROS levels and caspase-like activity and largely increases wild-type cell resistance to menadione. Although metacaspases can be kept inactive through S-nitrosylation, a recent publication showed that after activation, a second Cys residue that is conserved in all metacaspases can rescue the first S-nitrosylated site, rendering metacaspases even more active in a high ·NO environment (Belenghi *et al*., 2007). Our results are consistent with this mechanism, because we show that high ·NO production triggers ROS production that has been described to mediate metacaspase activation (Madeo *et al*., 1999, 2002).

Most interestingly, ·NO production in *btn1*-Δ cells is decreased both in physiological conditions and in response to menadione treatment. This ·NO synthesis defect in *btn1*-Δ cells is partially overcome by the addition of high L-arginine concentrations to the media. Furthermore, caspase-like activity can be increased and the resistance phenotype specifically reversed when *btn1*-Δ cells are treated with menadione in the presence of L-arginine. Because *btn1*-Δ cells are able to take up arginine from the media (Vitiello *et al*., 2007), this suggests that defective ·NO production in *btn1*-Δ cells is due to substrate limitation and that when *btn1*-Δ intracellular L-arginine levels are increased menadione-induced cell death is restored. Supporting the importance of Btn1p in menadione-induced cell death, we have observed a large viability increase when deleting *BTN1* in strains that are highly sensitive to menadione, such as *sod1*-Δ cells. As summarized in Figure 9, collectively these data indicate that the endogenous production of ·NO by *S. cerevisiae* cells seems to be required for oxidative stress induced active cell death. In particular, ·NO seems to be synthesized from L-arginine, increasing the production of ROS within the cell and inducing the activation of a cell death cascade. Furthermore, ·NO synthesis might be limited in *btn1*-Δ cells by low L-arginine levels, possibly blocking ROS production and metacaspase activation, causing an impairment of menadione-induced apoptosis.

In the context of Btn1p/CLN3 function, a recent study showed that disruption of Btn1p (*btn1*-Δ) alters coupling of the V-ATPase and proton-pumping across the vacuolar membrane (Padilla-Lopez and Pearce, 2006). This disruption in the electrochemical gradient between the cytosol and the vacuole likely underlies the decreased vacuolar transport of arginine observed in *btn1*-Δ strains. It is possible that Btn1p/CLN3 has a role in regulating intracellular levels of arginine through active regulation of vacuolar content. Importantly, these defects have been confirmed in human cell lines from JNCL patients (Ramirez-Montealegre *et al*., 2005) where it has been demonstrated that the absence of functional Cln3 results in defective lysosomal transport of L-arginine and in reduced intracellular L-arginine levels. By the use of the yeast model for JNCL, we have shown for the first time that mutations in BTN1/CLN3 cause an L-arginine–related limitation in ·NO synthesis both in physiological and oxidative stress conditions. This could be a relevant advance in our understanding of JNCL, because a defect in ·NO synthesis may contribute to the extensive neuronal death observed in the patients. Among other protective functions (for review, see Kang *et al*., 2004), ·NO synthesis was shown to inhibit the generation of the proapoptotic sphingolipid ceramide (De Nadai *et al*., 2000) that Puranam *et al*. (1997) found to be increased in the brains of JNCL patients. Therefore, defective ·NO synthesis might be the event in JNCL pathology that is causing ceramide accumulation and neuronal apoptosis. However, proving this hypothesis requires further studies targeted at in detail evaluation of ·NO signaling in more complex in vitro and in vivo JNCL model systems.

ACKNOWLEDGMENTS

We thank S. Phillips-Vitiello for critical reading of the manuscript and for technical assistance in the generation of the double deletion strains; Professors N. Sousa, J. Palha, and M. T. Silva for critical reading of the manuscript and helpful comments; D. Ramirez for help in the statistical analysis of the data; and J. Frade and R. Santos for technical assistance in the electrochemical experiments. We are also grateful to Professor M. Côrte-Real for enthusiasm in the beginning of this work. This work was supported by Fundação para a Ciência e a Tecnologia (FCT) grant POCI/BIA-BCM/57364/2004, PTDC/SAU-NEU/70161/2006, and National Institutes of Health grant R01 NS-36610. N.S.O., A.C., and A.J.A. are supported by scholarships from the FCT.

REFERENCES

Almeida, B., Sampaio-Marques, B., Carvalho, J., Silva, M. T., Leao, C., Rodrigues, F., and Ludovico, P. (2007). An atypical active cell death process underlies the fungicidal activity of ciclopirox olamine against the yeast *Saccharomyces cerevisiae*. FEMS Yeast Res. *7*, 404–412.

Beal, M. F., Ferrante, R. J., Browne, S. E., Matthews, R. T., Kowall, N. W., and Brown, R. H., Jr. (1997). Increased 3-nitrotyrosine in both sporadic and familial amyotrophic lateral sclerosis. Ann. Neurol. *42*, 644–654.

Belenghi, B., Romero-Puertas, M. C., Vercammen, D., Brackenier, A., Inze, D., Delledonne, M., and Van Breusegem, F. (2007). Metacaspase activity of *Arabidopsis thaliana* is regulated by S-nitrosylation of a critical cysteine residue. J. Biol. Chem. *282*, 1352–1358.

Boustany, R. M. (1992). Neurology of the neuronal ceroid-lipofuscinoses: late infantile and juvenile types. Am. J. Med. Genet. *42*, 533–535.

Boveris, A., Costa, L. E., Poderoso, J. J., Carreras, M. C., and Cadenas, E. (2000). Regulation of mitochondrial respiration by oxygen and nitric oxide. Ann. N Y Acad. Sci. *899*, 121–135.

Brune, B. (2005). The intimate relation between nitric oxide and superoxide in apoptosis and cell survival. Antioxid. Redox. Signal. *7*, 497–507.

Butterfield, D. A., Castegna, A., Lauderback, C. M., and Drake, J. (2002). Evidence that amyloid beta-peptide-induced lipid peroxidation and its sequelae in Alzheimer's disease brain contribute to neuronal death. Neurobiol. Aging *23*, 655–664.

Cassanova, N., O'Brien, K. M., Stahl, B. T., McClure, T., and Poyton, R. O. (2005). Yeast flavohemoglobin, a nitric oxide oxidoreductase, is located in both the cytosol and the mitochondrial matrix: effects of respiration, anoxia,

and the mitochondrial genome on its intracellular level and distribution. J. Biol. Chem. *280*, 7645–7653.

Castello, P. R., David, P. S., McClure, T., Crook, Z., and Poyton, R. O. (2006). Mitochondrial cytochrome oxidase produces nitric oxide under hypoxic conditions: implications for oxygen sensing and hypoxic signaling in eukaryotes. Cell Metab. *3*, 277–287.

Chen, S. R., Dunigan, D. D., and Dickman, M. B. (2003). Bcl-2 family members inhibit oxidative stress-induced programmed cell death in *Saccharomyces cerevisiae*. Free Radic. Biol. Med. *34*, 1315–1325.

Croopnick, J. B., Choi, H. C., and Mueller, D. M. (1998). The subcellular location of the yeast *Saccharomyces cerevisiae* homologue of the protein defective in the juvenile form of batten disease. Biochem. Biophys. Res. Commun. *250*, 335–341.

De Nadai, C., Sestili, P., Cantoni, O., Lievremont, J. P., Sciorati, C., Barsacchi, R., Moncada, S., Meldolesi, J., and Clementi, E. (2000). Nitric oxide inhibits tumor necrosis factor-alpha-induced apoptosis by reducing the generation of ceramide. Proc. Natl. Acad. Sci. USA *97*, 5480–5485.

Delafuente, J. M., Alvarez, A., Nombela, C., and Sanchez, M. (1992). Flow Cytometric analysis of *Saccharomyces cerevisiae* autolytic mutants and protoplasts. Yeast *8*, 39–45.

Dexter, D. T., Carter, C. J., Wells, F. R., Javoy-Agid, F., Agid, Y., Lees, A., Jenner, P., and Marsden, C. D. (1989). Basal lipid peroxidation in substantia nigra is increased in Parkinson's disease. J. Neurochem. *52*, 381–389.

Domitrovic, T., Palhano, F. L., Barja-Fidalgo, C., DeFreitas, M., Orlando, M.T.D., and Fernandes, P.M.B. (2003). Role of nitric oxide in the response of *Saccharomyces cerevisiae* cells to heat shock and high hydrostatic pressure. FEMS Yeast Res. *3*, 341–346.

Ferreira, N. R., Ledo, A., Frade, J. G., Gerhardt, G. A., Laranjinha, J., and Barbosa, R. M. (2005). Electrochemical measurement of endogenously produced nitric oxide in brain slices using Nafion/o-phenylenediamine modified carbon fiber microelectrodes. Anal. Chim. Acta *535*, 1–7.

Garg, H. S., Awasthi, Y. C., Neff, W. A., Ansari, N. H., and Srivastava, S. K. (1982). Studies in neuronal ceroid lipofuscinoses–enzymes of liver and brain-tissues involved in the defense against oxidative damage. J. Neurosci. Res. *7*, 305–311.

Gerasimenko, J. V., Gerasimenko, O. V., Palejwala, A., Tepikin, A. V., Petersen, O. H., and Watson, A.J.M. (2002). Menadione-induced apoptosis: roles of cytosolic Ca(2+) elevations and the mitochondrial permeability transition pore. J. Cell Sci. *115*, 485–497.

Goebel, H. H. (1995). The neuronal ceroid-lipofuscinoses. J. Child. Neurol. *10*, 424–437.

Goebel, H. H. (1997). Morphologic diagnosis in neuronal ceroid lipofuscinoses. Neuropediatrics *28*, 67–69.

Golabek, A. A., Kida, E., Walus, M., Kaczmarski, W., Michalewski, M., and Wisniewski, K. E. (2000). CLN3 protein regulates lysosomal pH and alters intracellular processing of Alzheimer's amyloid-beta protein precursor and cathepsin D in human cells. Mol. Genet. Metab. *70*, 203–213.

Good, P. F., Hsu, A., Werner, P., Perl, D. P., and Olanow, C. W. (1998). Protein nitration in Parkinson's disease. J. Neuropathol. Exp. Neurol. *57*, 338–342.

Gralla, E. B. (1997). Superoxide dismutase: studies in the yeast *Saccharomyces cerevisiae*. In: *Cold Spring Harbor Monograph Series*, *34*. *Oxidative Stress and the Molecular Biology of Antioxidant Defenses*, ed. J. G. Scandalios, Cold Spring Harbor Laboratory Press, Plainview, NY, 495–525.

Guarneri, R., Russo, D., Cascio, C., D'Agostino, S., Galizzi, G., Bigini, P., Mennini, T., and Guarneri, P. (2004). Retinal oxidation, apoptosis and age- and sex-differences in the mnd mutant mouse, a model of neuronal ceroid lipofuscinoses. Brain Res. *1014*, 209–220.

Guo, F. Q., Okamoto, M., and Crawford, N. M. (2003). Identification of a plant nitric oxide synthase gene involved in hormonal signaling. Science *302*, 100–103.

Jolly, R. D., Brown, S., Das, A. M., and Walkley, S. U. (2002). Mitochondrial dysfunction in the neuronal ceroid-lipofuscinoses (Batten disease). Neurochem. Int. *40*, 565–571.

Kanadia, R. N., Kuo, W. N., Mcnabb, M., and Botchway, A. (1998). Constitutive nitric oxide synthase in *Saccharomyces cerevisiae*. Biochem. Mol. Biol. Int. *45*, 1081–1087.

Kang, Y. C., Kim, P. K., Choi, B. M., Chung, H. T., Ha, K. S., Kwon, Y. G., and Kim, Y. M. (2004). Regulation of programmed cell death in neuronal cells by nitric oxide. In Vivo *18*, 367–376.

Kim, Y., Ramirez-Montealegre, D., and Pearce, D. A. (2003). A role in vacuolar arginine transport for yeast Btn1p and for human CLN3, the protein defective in Batten disease. Proc. Natl. Acad. Sci. USA *100*, 15458–15462.

Lassmann, H., Bancher, C., Breitschopf, H., Wegiel, J., Bobinski, M., Jellinger, K., and Wisniewski, H. M. (1995). Cell death in Alzheimer's disease evaluated by DNA fragmentation in situ. Acta Neuropathol. *89*, 35–41.

Ledo, A., Barbosa, R. M., Frade, J., and Laranjinha, J. (2002). Nitric oxide monitoring in hippocampal brain slices using electrochemical methods. Nitric Oxide *359*, 111–125.

Lerner, T. J. *et al*. (1995). Isolation of a novel gene underlying batten-disease, Cln3. Cell *82*, 949–957.

Ludovico, P., Rodrigues, F., Almeida, A., Silva, M. T., Barrientos, A., and Corte-Real, M. (2002). Cytochrome c release and mitochondria involvement in programmed cell death induced by acetic acid in *Saccharomyces cerevisiae*. Mol. Biol. Cell. *13*, 2598–2606.

Ludovico, P., Sansonetty, F., and Corte-Real, M. (2001). Assessment of mitochondrial membrane potential in yeast cell populations by flow cytometry. Microbiology *147*, 3335–3343.

Madeo, F., Frohlich, E., Ligr, M., Grey, M., Sigrist, S. J., Wolf, D. H., and Frohlich, K. U. (1999). Oxygen stress: a regulator of apoptosis in yeast. J. Cell Biol. *145*, 757–767.

Madeo, F. *et al*. (2002). A caspase-related protease regulates apoptosis in yeast. Mol. Cell *9*, 911–917.

Marklund, S. L., Santavuori, P., and Westermarck, T. (1981). Superoxide-dismutase, catalase and glutathione-peroxidase in infantile, late infantile and juvenile neuronal ceroid-lipofuscinoses. Clin. Chim. Acta *116*, 191–198.

McCord, J. M., and Fridovich, I. (1969). Superoxide dismutase. An enzymic function for erythrocuprein (hemocuprein). J. Biol. Chem. *22*, 6049–6055.

Mochizuki, H., Goto, K., Mori, H., and Mizuno, Y. (1996). Histochemical detection of apoptosis in Parkinson's disease. J. Neurol. Sci. *137*, 120–123.

Morrison, M. H., Jernstrom, B., Nordenskjold, M., Thor, H., and Orrenius, S. (1984). Induction of DNA damage by menadione (2-methyl-1,4-naphthoquinone) in primary cultures of rat hepatocytes. Biochem. Pharmacol. *33*, 1763–1769.

Munroe, P. B. *et al*. (1997). Spectrum of mutations in the Batten disease gene, CLN3. Am. J. Hum. Genet. *61*, 310–316.

Nogae, I., and Johnston, M. (1990). Isolation and characterization of the Zwf1 gene of *Saccharomyces cerevisiae*, encoding glucose-6-phosphate-dehydrogenase. Gene *96*, 161–169.

Ohsumi, Y., Kitamoto, K., and Anraku, Y. (1988). Changes induced in the permeability barrier of the yeast plasma-membrane by cupric ion. J. Bacteriol. *170*, 2676–2682.

Packer, M. A., Porteous, C. M., and Murphy, M. P. (1996). Superoxide production by mitochondria in the presence of nitric oxide forms peroxynitrite. Biochem. Mol. Biol. Int. *40*, 527–534.

Padilla-Lopez, S., and Pearce, D. A. (2006). Saccharomyces cerevisiae lacking Btn1p modulate vacuolar ATPase activity to regulate pH imbalance in the vacuole. J. Biol. Chem. *15*, 10273–10280.

Pearce, D. A., Carr, C. J., Das, B., and Sherman, F. (1999a). Phenotypic reversal of the btn1 defects in yeast by chloroquine: a yeast model for Batten disease. Proc. Natl. Acad. Sci. USA *96*, 11341–11345.

Pearce, D. A., Ferea, T., Nosel, S. A., Das, B., and Sherman, F. (1999b). Action of BTN1, the yeast orthologue of the gene mutated in Batten disease. Nat. Genet. *22*, 55–58.

Pearce, D. A., McCall, K., and Chattopadhyay, S. (2003). Altered amino acid levels in sera of a mouse model for juvenile neuronal ceroid lipofuscinoses. Clin. Chim. Acta *332*, 145–148.

Pearce, D. A., Nosel, S. A., and Sherman, F. (1999c). Studies of pH regulation by Btn1p, the yeast homolog of human Cln3p. Mol. Genet. Metab. *66*, 320–323.

Pearce, D. A., and Sherman, F. (1997). BTN1, a yeast gene corresponding to the human gene responsible for Batten's disease, is not essential for viability, mitochondrial function, or degradation of mitochondrial ATP synthase. Yeast *13*, 691–697.

Pearce, D. A., and Sherman, F. (1998). A yeast model for the study of Batten disease. Proc. Natl. Acad. Sci. USA *95*, 6915–6918.

Pedersen, W. A., Fu, W., Keller, J. N., Markesbery, W. R., Appel, S., Smith, R. G., Kasarskis, E., and Mattson, M. P. (1998). Protein modification by the lipid peroxidation product 4-hydroxynonenal in the spinal cords of amyotrophic lateral sclerosis patients. Ann. Neurol. *44*, 819–824.

Postma, E., Verduyn, C., Scheffers, W. A., and Vandijken, J. P. (1989). Enzymic analysis of the crabtree effect in glucose-limited chemostat cultures of *Saccharomyces cerevisiae*. Appl. Environ. Microbiol. *55*, 468–477.

Puranam, K., Qian, W. H., Nikbakht, K., Venable, M., Obeid, L., Hannun, Y., and Boustany, R. M. (1997). Upregulation of Bcl-2 and elevation of ceramide in Batten disease. Neuropediatrics *28*, 37–41.

Ramirez-Montealegre, D., and Pearce, D. A. (2005). Defective lysosomal arginine transport in juvenile batten disease. Hum. Mol. Genet. *14*, 3759–3773.

Smith, M. A., Richey Harris, P. L., Sayre, L. M., Beckman, J. S., and Perry, G. (1997). Widespread peroxynitrite-mediated damage in Alzheimer's disease. J. Neurosci. *17*, 2653–2657.

Thor, H., Smith, M. T., Hartzell, P., Bellomo, G., Jewell, S. A., and Orrenius, S. (1982). The metabolism of menadione (2-methyl-1,4-naphthoquinone) by isolated hepatocytes. A study of the implications of oxidative stress in intact cells. J. Biol. Chem. *257*, 12419–12425.

Vachova, L., and Palkova, Z. (2005). Physiological regulation of yeast cell death in multicellular colonies is triggered by ammonia. J. Cell Biol. *169*, 711–717.

Vitiello, S. P., Wolfe, D. M., and Pearce, D. A. (2007). Absence of Btn1p in the yeast model for juvenile Batten disease may cause arginine to become toxic to yeast cells. Hum. Mol. Genet. *16*, 1007–1016.

Zamzami, N., Marchetti, P., Castedo, M., Decaudin, D., Macho, A., Hirsch, T., Susin, S. A., Petit, P. X., Mignotte, B., and Kroemer, G. (1995). Sequential reduction of mitochondrial transmembrane potential and generation of reactive oxygen species in early programmed cell death. J. Exp. Med. *182*, 367–377.